Journal of the European Ceramic Society 22 (2002) 1–13

www.elsevier.com/locate/jeurceramsoc

Lithographic printing of ceramics

Nigel S. Leyland [a], Julian R.G. Evans [a,*], David J. Harrison [b]

[a] *Department of Materials, Queen Mary and Westfield College, University of London, Mile End Road, London E1 4NS, UK*
[b] *Department of Design, Brunel University, Runneymede Campus, Englefield Green, Egham TW20 0JZ, UK*

Received 30 November 2000; received in revised form 23 February 2001; accepted 4 March 2001

Abstract

The broad aim of this paper is to explore the potential and limitations of offset lithogaphy for a wide range of hitherto unrecognised applications in materials processing. Lithographic printing of metal powders provides a rapid manufacturing pathway for the production of circuit tracks. The ability to superimpose functional ceramic inks by multiple registration would confer a capability to add on-board sensors, sounders, actuators and other discrete components. In order to take full advantage of this high speed printing technology and apply it generally to ceramic and metal powders, perhaps in combination with polymer films, the range of acceptable ink properties needs to be defined and the ink properties must be related to print quality and to characteristic print defects. In this investigation, a range of lithographic inks containing ascending TiO_2 volume fractions and a selection of dispersants was formulated and tested. The flow properties and emulsion characteristics were related to the quality of deposition in a conventional, single-colour, automatic lithographic press.

Keywords: Inks; Lithographic printing; Multilayer devices; Print quality; Rheology; TiO_2

1. Introduction

In the quest for alternatives to compaction methods of assembling ceramic particles, manufacturing pathways have been acquired from a range of industries that have no formal connection with ceramics. In many of these processes, particles are dispersed in an organic vehicle, the properties of which play a part in conferring shape. Operations brought in from the paint[1] and printing[2–4] industries are particularly interesting because they allow the creation of a three dimensional shape by point, line or planar addition of material and therefore, classify as solid freeforming processes. This means that shape and in some cases, the three dimensional spatial arrangement of microstructure can be controlled from a computer file.[5] Screen printing has become well established in the manufacture of capacitors and multi-layer ceramic devices.[6] Ink jet printing of ceramic binder[7] onto layers of ceramic powder provides a way of creating extremely complex shapes for foundry cores and moulds. Direct inkjet printing can produce ceramic components by deposition of a well-dispersed suspension through the nozzles of continuous,[3,8,9] or drop on demand[4,10–13] inkjet printers. In this way, micro-cavities[14] and continuous functional gradients[5] can be produced. Xerography has been used for solid freeforming of metal powder[15] yielding what could be described as a ''manufacturing photocopier''. It has been argued that there is a case to explore all printing technologies as potential solid freeforming pathways.[14]

The lithographic deposition of conducting metal-filled inks has been used as an alternative to copper-phenolic printed circuits[16–18] where it allows very high speed manufacturing and provides circuits on a wide range of flexible substrates. It has been proved effective in the manufacture of microwave integrated circuits[19] and analogue filters.[20]

Reprographic lithography is the process of printing from a plane surface on which the printing areas are oleophilic and, therefore, pick up ink from the inking roller while the non-printing areas are hydrophilic and are maintained in a damp condition by the fountain solution.[21] The process should not be confused with electron beam lithography or stereolithography which have some similarity to modern lithographic plate production methods because they involve masking or photo-curing of

* Corresponding author. Tel.: +44-20-7882-5501; fax: +44-20-8981-9804.
E-mail address: j.r.g.evans@qmw.ac.uk (J.R.G. Evans).

0955-2219/01/$ - see front matter
PII: S0955-2219(01)00247-3

polymers and have ambiguously acquired the title "lithography" but they are to be differentiated from the high speed printing process correctly named lithography and described in this paper.

The conductive lithographic film (CLF) process[16–20] which is now well established would benefit from being augmented by the capability to register and overprint functional ceramics in order to provide on-board sensors, piezoelectric actuators, sounders or simply capacitors. In some of these applications, sufficient performance could be obtained from a highly filled 0–3 ceramic–polymer composite, defined by Newnham's contiguity classification.[22] in which the polymer was used as the organic ink vehicle. In another approach, the high speed of lithography may become competitive with other printing operations in the preparation of discrete components intended for subsequent sintering.

Guidelines for the formulation and preparation of ceramic inks need to be addressed, as do the procedures for assessing emulsification behaviour [23] and for dealing with transient effects in rheometry.[24] Of particular interest are the following questions. What are the upper and lower limits for ink viscosity? Which dispersants are effective? Can ink emulsification be controlled at high filler loadings? A separate series of questions relate to the quality of the printed image. What is the print resolution defined both one-dimensionally in terms of line gap and two-dimensionally in terms of hole width? What are the dot and line gains? What are the smallest printable image shapes and dimensions? What is the minimum line width that preserves continuity? These are issues that relate particularly to the miniaturisation of circuits. Are large print areas continuous, that is, free from 'pin holes'? This is important in the deposition of insulating layers.

Many laboratory tests have been devised to characterise reprographic inks in terms of viscosity, tack and water pick-up. Tack is defined as a measure of the force required to split a single film of ink into two.[21] It is influenced by adhesive behaviour and transient viscosity. In a recent assessment of these, Volz [25] testifies to the complexity of the lithographic process and assertively argues that inks should be evaluated on a small duplicator press. The present authors recognise the sagacity of this advice and adopt such a testing protocol in this work.

The aim of the present work is to explore these issues for ceramic deposition by offset lithography in an attempt to set in place the guidelines for the generic deployment of lithography in materials processing.

2. Experimental procedure

Details of the materials used are given in Table 1. The titania powder was an uncoated rutile, milled as a pigment precursor, having an ultimate particle size in the 200 nm region, as revealed by TEM. The commercial ink used for comparison was an air-drying acrylic, oil-based glossy black. A commercial air-drying lithographic varnish, based on a mixture of linseed and tung oils donated by Coates Lorilleux was used as the main component of the vehicle. In some cases, this was diluted with a high boiling point (180–210°C) petroleum distillate solvent giving a typical commercial lithographic printing vehicle-solvent system. The dispersants studied were Solsperse 3000, 13940 and 17940 and were selected on the basis of the manufacturer's recommendations as suitable for the dispersion of inorganic pigments in organic resins, including lithographic inks and specifically titania pigmented paints.

In all cases, dispersants were added at the manufacturer's recommended level of 2 mg of dispersant per square metre of ceramic powder surface, as deduced from BET nitrogen adsorption by the powder supplier. Varnish-solvent mixtures were prepared to establish the viscosity-composition relationship. For the preparation of ceramic ink, the varnish was diluted with solvent in the mass ratio of 4:1 and the dispersant was added. The powder was progressively stirred in over a period of several minutes to produce a slurry, or in the case of inks above 37 vol.%, a crumble. The inks were then milled for 10 min on a triple roll mill with rolls of length 400 mm and diameter 150 mm (ex-Cox Machines Ltd, Bristol, UK) with roll surface speeds of 0.21, 0.6 and

Table 1
Details of Materials

Description	Grade	Supplier	Density/kg m^{-3}
Ceramic powder	RSM3	Tioxide Ltd, Stockton on Tees, UK	4260
Commercial black ink	VS103 Infinity Black	Van Son Ink Corp^{n}, Mineola, NY, USA	–
Formulated varnish	XY39 High gloss	Coates Lorilleux Ltd, St Mary, Cray, Kent, UK	946
Diluent	PKWF4/7	Halterman Ltd, Barnet, UK	810
Dispersant	Solsperse 3000	Zeneca Ltd, Manchester, UK	910
Dispersant	Solsperse 13940	Zeneca Ltd, Manchester, UK	818[a]
Dispersant	Solsperse 17940	Zeneca Ltd, Manchester, UK	860[a]
Fountain	V2020	Van Son Ink Corp^{n}, Mineola, NY, USA	–

[a] In hydrocarbon solvent at 40% by mass.

Table 2
Composition of titanium dioxide inks

Ink formulation	Dispersant grade	TiO_2 (wt.%)	Varnish (wt.%)	Solvent (wt.%)	Dispersant (wt.%)	TiO_2 (vol.%)		
						As printed		Dried (from drying test)
						Intended	From ashing	
A	13940	67.05	26.67	5.33	0.94	30	31	47
B	17940	67.05	26.67	5.33	0.94	30	30	47
C	3000	67.05	26.67	5.33	0.94	30	28	44
D	3000	67.05	25.61	6.4	0.94	30	30	47
E	3000	71.54	21.97	5.49	1.00	35	35	53
F	3000	72.75	20.97	5.24	1.02	37	37	55
G	3000	75.20	19.00	4.75	1.05	40	39	57
H	3000	78.82	16.06	4.02	1.10	45	43	61

1.53 m s^{-1} (feed to exit). They were stored in sealed containers. The ceramic ink compositions are given in Table 2. Solvent incorporated in the as-received dispersant was included as part of the diluent. These solvents are very similar; that in the dispersant has a boiling point of 240–280°C and the diluent 240–270°C.

Inks A, B and C were prepared in order to test the effectiveness of the dispersants and were based on a modest 30 vol.% ceramic loading. Inks D–G were formulated after screening the dispersants and are based on volume fractions of ceramic judged to span the range of viscosity acceptable for printing. An ink based on the commercial black was prepared by blending with 10 wt.% diluent in order to match the viscosity of ceramic ink C. Ceramic inks were mixed with 1 wt.% of the commercial black at the ink fountain to enhance visibility.

The weight fraction of ceramic in the inks was confirmed by loss on ignition, in which weighed samples (approximately 15 g) of ink were heated to 600°C in air before re-weighing. Drying tests were carried out at 150°C to constant mass on films approximately 100 μm thick for the formulated varnish and the ceramic inks (Table 2).

The viscosity of the diluent was measured using a size 1 certificated, suspended level, reverse flow glass viscometer (BS/1P/RF) following the procedure recommended in BS188:1977 at a temperature of 25°C. The viscosity of diluent-varnish mixtures was measured using a Haake RS150, as described below at shear rates in the range 0.03–20 s^{-1}. Each data point was collected after holding the sample at constant shear rate for 20 ks.

Rheological characterization of the inks was performed on a Haake RS150 cone and plate rheometer using a cone of diameter 35mm and opening angle 2 at 25±0.6°C maintained by a circulating oil heater. Data were collected at constant shear rates in the range 0–20 s^{-1}. Unless otherwise stated, the ink samples were sheared at constant strain rate for a period of 10.8 ks in order to extinguish the effects of thixotropy and to allow the samples to reach the steady state. Reliable data were collected by recording the mean value of shear stress over the last 1 ks. The need for this protocol was demonstrated by collecting data from the same samples using rapid sweeps. Some inks were tested using a Davenport capillary rheometer fitted with a 1 mm diameter, 40 mm long die and a 5000 psi (34 MPa) transducer. Since the length: diameter ratio was 40, the Bagley correction was not applied. The Rabinowitsch correction was applied.

The sizes of agglomerates in the inks were measured using a Hegman gauge (Pearson Panke Equipment Ltd, London, UK). The largest intrinsic agglomerate size was defined as the point in the gauge depth scale at which a large number of scratches appeared simultaneously across the ink film in the channel. A mean value was calculated from the results of four sweeps.

The emulsion behaviour of the ceramic inks A–G and the commercial black ink, both as-received and diluted with 10% diluent were assessed using Surland's method.[23] Samples of 100 g fountain solution and 100 g ink were stirred for 60 s at 100 rpm. Excess fountain was decanted and measured before returning it to the stirrer. Water pick-up was plotted as a function of time over a total stirring time of 600 s. Printing was performed on a Multilith 1250 offset lithographic printing press (AM Corporation, Mount Prospect, Illinois, USA) and test patterns were printed onto 115 gm^{-2} gloss art paper. The printing press is shown schematically in Fig. 1. Patterns on the printing plate (Fig. 2) were chosen to test resolution of both minimum line thickness and minimum separation, line continuity, area coverage, angular reproduction, dot and line gain, and registration. The test pattern was designed using Adobe Illustrator 8.0 running on an IBM compatible PC. Plates were produced from this software by a negative process, a process which provides slightly higher gain than a positive method because of diffraction and collimation effects.

The blanket to plate pressure was set to give an unbroken line 5 mm in width from a completely inked plate. The blanket to impression cylinder pressure was

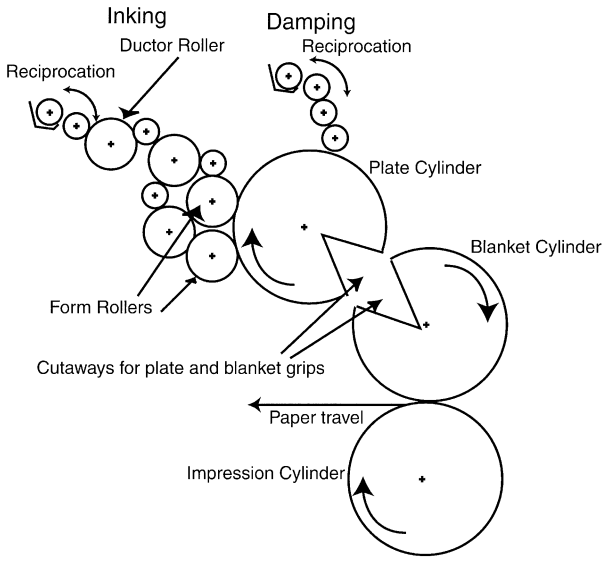

Fig. 1. Schematic diagram of the Multilith 1250 lithographic printing press.

set to just grip the paper. A minimum speed (5000 impressions per hour) was selected. For each ink, the fountain and ink supply were adjusted to give optimum image quality as gauged by observation. The manufacturer's recommended procedure was used to adjust registration.

Multiple layers were built up by repeated overprinting without drying, to produce test pages with up to ten layers of ink, to determine both the accuracy of print registration and the stability of the ink films during overprinting. Overprinting was also performed on test pages, which were allowed to dry overnight between the printing of each layer. Up to ten layers of ink were printed.

The printed test sheets were examined by optical microscopy in transmitted light under conditions of bright field illumination and measurements were made with the aid of an on-stage graticule. Area measurements were made using an Olympus BX60 image analysis microscope (Olympus Optical Co., Tokyo, Japan) and Image-Pro Plus analysis software (Media Cybernetics, Silver Spring, MD, USA) in transmitted light, which was found to eliminate artefacts caused by paper surface features. A Jeol JSM 6300 scanning electron microscope was used to study the ink deposit and secondary electron images were acquired from carbon coated samples.

3. Results and discussion

3.1. Ink viscosity

As a first step in the formulation of ceramic inks, viscosity in the diluent-varnish system was assessed (Fig. 3). The suspended level viscometer, used for the diluent, imposes low shear rates (<1 s^{-1}) and so comparable low shear rate values from the cone and plate viscometer were taken for the solutions. These exhibit only slight shear thinning in the shear rate range studied (0.03–20 s^{-1}) and so the values given approximate to the zero shear rate viscosities.

A number of equations have been proposed for the viscosity of liquid mixtures including:[26]

$$\eta^{1/3} = x_1\eta_1^{1/3} + x_2\eta_2^{1/3} \quad (1)$$

where x is mole fraction and subscripts 1 and 2 refer to solvent and solute respectively. As an alternative, the following equations have been used[27,28]

$$\ln\eta = x_1\ln\eta_1 + x_2\ln\eta_2 \quad (2)$$

$$\ln\eta = v_1\ln\eta_1 + v_2\ln\eta_2 \quad (3)$$

$$\ln\eta = \frac{1}{2}(x_1 + v_1)\ln\eta_1 + \frac{1}{2}(x_2 + v_2)\ln\eta_2 \quad (4)$$

where v is volume fraction. Other equations use solution enthalpies[28] or empirical constants that are specific to a given system.[29] Fig. 3 shows that Eq. (2) best describes the variation of viscosity with composition at the varnish-rich end of the system. Solvent-rich compositions (<70 wt.% varnish) were not measurable on the cone and plate rheometer. These compositions formed emulsions of a dispersed varnish-rich phase that underwent significant coarsening in the suspended level viscometer. Observation of thin films of varnish-rich mixtures, containing 80 wt.% or more varnish, by optical microscopy in transmitted light revealed that they were also emulsions, with spheroidal droplets of a diluent-rich phase dispersed in the varnish. The miscibility of these two components is limited but such phase separation does not impede their commercial use in combination.

Diluent reduces the viscosity and increases ceramic volume fraction from the printed to the dried condition, as solvent evaporates (Table 2). The use of large amounts of solvent should enable high ceramic volume fractions to be deposited, but large solvent additions also interfere with drying of the ink varnish. In subsequent work, 17 wt.% was used in inks for testing dispersants and 20 wt.% was used in inks intended for printing trials. The drying tests show that the formulated vehicle contained 32 wt.% of volatile material, including that already present in the varnish (Table 2). This means that dried inks contain sinterable volume fractions of ceramic (50–60 vol%).

Inks A–C which contain different dispersants at the same level of addition (2 mg m^{-2}), displayed quite different behaviour on the triple roll mill. Ink A produced a thick dough. Ink B was more fluid and consistent with a reprographic ink while C was very fluid, difficult to contain on the rolls and clearly offered scope for increased ceramic

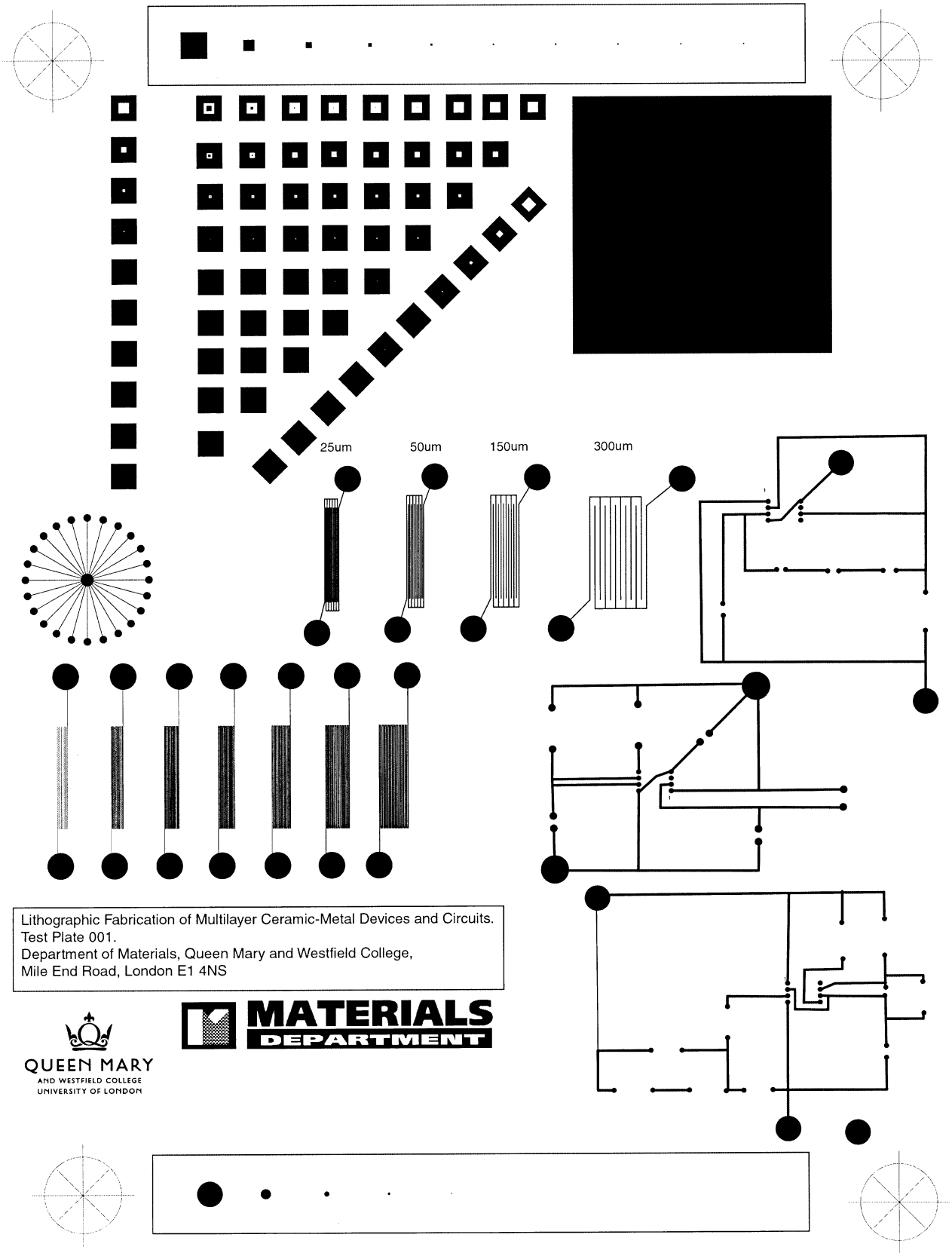

Fig. 2. The print test pattern (image area A4: 297×210 mm).

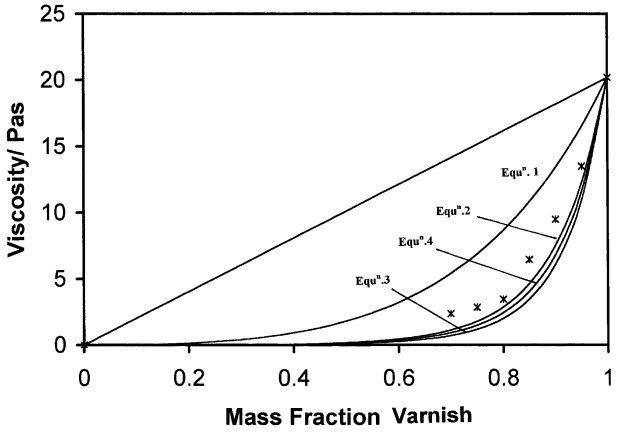

Fig. 3. Viscosity-composition plot in the binary diluent-varnish system compared with model equations for the viscosity of binary mixtures and gravimetric law of mixtures (straight line).

loading. Solsperse 3000, the dispersant contained in this ink is a poly (12-hydroxystearic acid), of molecular weight 1368, the structure being:

$$C_{12}H_{35}\text{-}CO\text{-}(O\text{-}C_{11}H_{21}\text{-}CO\text{-})_3\text{-}O\text{-}C_{11}H_{21}\text{-}COOH$$

$$\begin{array}{cc} | & | \\ C_5H_{11} & C_5H_{11} \end{array}$$

The single–COOH carboxylic acid functional group is thought to attach to the ceramic surface; infra-red spectroscopy of similar acid-terminated dispersants on zirconia show acid-base behaviour.[30] High particle surface coverage per molecule of dispersant is achieved by the branched chain structure.[31] In contrast, the dispersant used in ink A was a comb-structure copolymer with an amine anchoring group on each chain. That used in ink B was a single chain polymer with an amine group. TiO_2 is sometimes reported to have an isoelectric point of surface just below 7, prompting the selection of amine-terminated dispersants. The fact that the acid-terminated dispersant showed distinctly higher fluidity on the mill, confirmed by viscosity measurement (vide infra) indicates that for oxide surfaces close to neutral pH, dispersant selection is not facile. Behaviour on the mill is reflected in the measured flow properties given below.

The degree of dispersion as assessed by a Hegman gauge or 'draw down' test is shown in Table 3. These sizes represent the depths of multiple score marks in a calibrated, wedge-shaped channel. The appearance of a small number of scratches at larger particle sizes was noted but attributed to extrinsic sources, including atmospheric dust, debris incorporated into the inks during manufacture, or a small residuum of larger agglomerates not fully dispersed during milling. The need for caution in interpreting such results is recognised within the ink-making profession.[32] The mean maximum intrinsic agglomerate sizes of the commercial black inks VS103 and VS102 were recorded as 3 and 4.8 μm, respectively. This concurs with information from the manufacturer, namely that smooth printed films of these inks are typically 2–4 μm thick[33] and confirms the Hegman gauge technique.

Table 3
Largest intrinsic agglomerate diameter as detected by hegman gauge draw-down tests (average of four tests)

Ink	Diameter (μm)	
	Mean	S.D.[a]
VS 102 black	3	0.9
VS103 black	5	0.5
A	9.5	0.9
B	7	0.4
C	5.5	0.2
D	8.6	1.0
E	8.5	1.1
F	11	0.9

[a] S.D. standard deviation.

The mean maximum intrinsic agglomerate sizes of inks A, B and C decrease with the viscosity (vide infra) apparently correlating the fluidity of the ink with the degree of dispersion of the ceramic phase and hence with the efficacy of the dispersant. The maximum agglomerate size increased with increasing ceramic loading, in the sequence of inks D–F, again correlating with increasing viscosity. The maximum agglomerate size for ceramic inks was only slightly greater than that of the commercial reprographic inks.

Ink F was too viscous to leave a trace in the gauge below 6μm. Ink G formed beads at channel depths below 20 μm and ink H did not draw down the channel at any point, forming a mass which was pushed in front of the blade. Agglomerate sizes could not be measured for inks G and H by this method.

The viscosities of inks A–C were used to select the dispersant. Although the transient viscosity at 300 s gives a reasonable approximation to steady state viscosity, it is actually too short for complete equilibrium as discussed below. It provides an explicit ranking of the inks containing different dispersants which are otherwise compositionally identical (Fig. 4). The apparent flow behaviour indices are similar at shear rates below 10 s^{-1} but the effect of different dispersants was to provide a range of one order of magnitude in viscosity. Ink A displayed stronger shear-thinning behaviour at high shear rates. These viscosity results confirm the observations made at the milling stage and form the basis for selecting Solsperse 3000. The flow behaviour index of ink C also matches most closely that of the commercial black ink, which has a higher viscosity over the shear rate range studied. Dilution of the commercial black ink reduces its viscosity by a factor of approximately 3 at a shear rate of 1 s^{-1}, but this became less pronounced at higher shear rates.

In the lithographic process, ink experiences very high shear rates in the inking roller train and in the transfers between plate, blanket and substrate.[34] In the Multilith press used here, nip shear rates were calculated to be in the range from approximately 4000 s^{-1} to approximately 500,000 s^{-1}, using the equation below[35]

$$\dot{\gamma} = \dot{\gamma}_1 + \dot{\gamma}_2 = \frac{3v\lambda^2}{H_0} + \frac{v_2 - v_1}{2H_0} \quad (5)$$

in which $\dot{\gamma}_1$, $\dot{\gamma}_2$ are the entrance and exit nip shear rates, v_1 and v_2 are the roll surface speeds, H_0 is half the nip width and λ is the material's die swell ratio, which for these inks is close to unity. The multilith's rolls alternate between being driven and idling, so consecutive roll surface speeds are equal, being approximately 0.7 m s^{-1}. A value of 4 μm was used for the final value of H_0, based on the printed film thickness, rising to 500 μm at the nip between the ductor roller and the first idling roller, assuming uniform and symmetrical ink splitting for an inking train containing seven rollers.

It is sometimes argued that for this reason viscosity should be assessed at high shear rates but the effects of cavitation, well known in cone and plate rheometry [24,36–38] gave an upper limit of about 50 s^{-1}. For higher shear rates, capillary rheometry was used. In contrast, the recovery of the ink film on the substrate, which takes place under the influence of surface and interfacial tensions and affects spreading, area coverage and the healing of pin holes, occurs at very low shear rates where yield stress is influential.

Some of the difficulties in recording a viscosity on materials that present both thixotropy and a long relaxation time have been discussed elsewhere.[24,37–43] In these systems, the flow behaviour is related to the formation of large weak agglomerates which break down at higher shear rates. Low shear-rate rhoepexy is a characteristic of the formation of these agglomerates. Similar problems are encountered in printing inks and this partly accounts for the paucity of published data on litho inks. Ink D was also tested under conditions where steady state viscosity was recorded (Fig. 5) on the cone and plate rheometer. Ink E suffered cavitation before steady-state flow was achieved and was tested at higher shear rates in the capillary rheometer, as were the series of inks F–G. The missing data from Fig. 5 are significant: ink H (45 vol.%) would not pass the rheometer and would not print, in contrast to ink G (40 vol.%), which passed easily through the press and the rheometer. These results are shown in Fig. 5 and represent a family of inks differing only in ceramic volume fraction. The data in Fig. 5 are discussed later in terms of the print quality and emulsification behaviour.

The results of the Surland water pick-up test are shown in Fig. 6. The test forms a fountain-in-ink emulsion and the water pick-up by ink is partly related to the interfacial area so created, which is strongly influenced by viscosity as well as the polarity of the ink vehicle. The results in Fig. 6 have been corrected to give uptake based on organic vehicle only. It can be seen that none

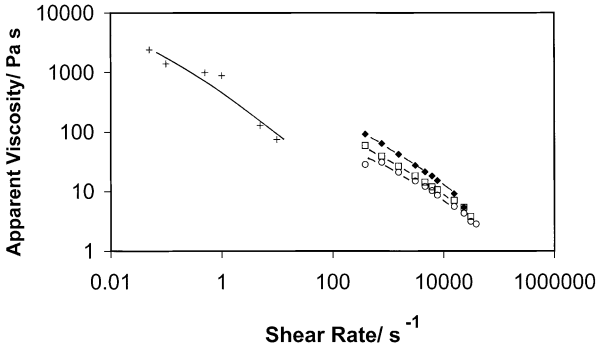

Fig. 5. Flow curves for inks of volume fraction 30–40 vol.% TiO_2 (D (+), E (○), F (□) and G (◆): Table 2), collected after 300 s at 0.05–10 s^{-1} and by capillary rheometry at 250–2500 s^{-1} (Rabinowitsch correction applied).

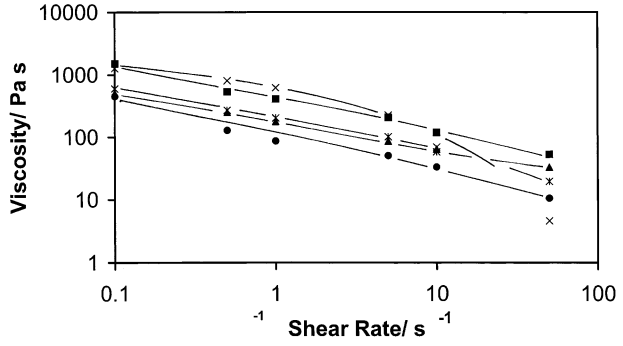

Fig. 4. Flow curves for commercial black ink (■), black ink diluted with 10 wt.% diluent (▲) and ceramic inks A (×), B (⋆) and C (●) with different dispersants at 30 vol.% TiO_2 loadings obtained from the cone and plate rheometer by collecting data at constant shear rate after 300 s.

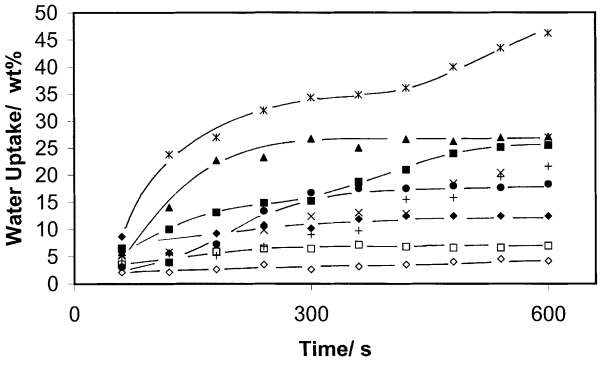

Fig. 6. Fountain pick-up curves for ceramic inks A (×), B ⋆), C (●), D (+), E (○), F (□) and G (◆), and commercial black ink as-received, (■) and diluted with 10 wt.% diluent (▲), based on ink vehicle mass only.

of the ceramic inks displays emulsification properties resembling those of the commercial black ink. All of the ceramic inks apart from A and B absorb significantly less fountain than does the commercial black ink and neither attain equilibrium during the test. The other ceramic inks do attain equilibrium, in that they do not absorb further fountain solution after the mid-point of the test, though this is at too low a concentration to be the result of saturation of the vehicle. The low water pick-up of the other ceramic inks is largely the result of their higher viscosity. This prevents break-up and dispersion of the ink in the continuous fountain phase and hence prevents exposure of fresh ink surface to the fountain. Inks E, F and G were too viscous to be broken up significantly and so exposed only a small surface area to the fountain solution. A more powerful stirrer motor would have provided no advantage for the degree of mixing. An acknowledged drawback of the Surland test is that it investigates water take-up only at low shear rates, while much higher shear rates are experienced on the plate, blanket and paper surfaces.[44] This is particularly significant for the strongly shear-thinning ceramic inks investigated here. Water pick up characteristics on the press may differ markedly from those in the test; thus, the emulsification characteristics of the ceramic and commercial inks may be much more similar during printing than they are in the test. These emulsification tests, along with ink viscosity, are discussed in relation to print quality in Section 3.2.

3.2. Printing trials

Test images were printed successfully using the undiluted commercial black ink and ceramic inks E, F and G (Table 2). Attempts to print using ink C which was very fluid (26 Pa s at 40 s^{-1}) were unsuccessful. The ink formed a scum, completely coating the surface of the printing plate with an ink-fountain emulsion during the inking process, before an impression could be made. No level of adjustment to the ink and fountain settings could render a useable image on the plate. This emulsion was extremely fluid and highly mobile under press conditions. Significant quantities of the emulsion were transferred onto the fountain damping roller during attempts to produce a stable image on the plate, necessitating the complete stripping and cleaning of the damping system. This result can be attributed either to its low viscosity or to enhanced affinity for water, perhaps due to the effective dispersant. To decide this issue, commercial black ink was diluted with solvent to give a viscosity of 21 Pa s at 40 s^{-1} which is comparable to the viscosity of ink C (26 Pa s at 40 s^{-1}). The flow curves of the diluted and undiluted commercial inks are shown for comparison with ceramic inks A–C in Fig. 4. The diluted commercial ink gave identical problems; the plate and damping system became scummed by an inverted ink-in-fountain emulsion. These results suggest that, as a guide, the lower limit of ink viscosity, for ceramic lithography is about 26 Pa s at 40 s^{-1}. A parallel criterion can be deduced from the Surland test. Here it is not just the saturation level which should be below 45%, but also the time at which saturation occurs which should not be below 300 s.

A surprising feature of the printing experiments was that inks which appeared to be too rigid to load into the ink fountain could nevertheless be printed. The reason is that at high shear rates, the viscosities are similar (Fig. 5). The commercial black ink and ceramic inks C and E could be placed conventionally in the ink fountain with a pallet knife. Inks F and G, being more rigid, were rolled out into a bar by hand before being placed in the nip of the ink fountain, and then transferred to the rollers. Ink H was too rigid to be formed in this way, or to be taken up by the inking rollers and printing was not attempted.

The ink and fountain settings used for those inks which printed successful test pages are given in Table 4. The ink and fountain settings refer to the degrees of arc for which the inking and fountain rollers respectively make contact with ductor rollers on each revolution.

Printed areas in black ink and inks E and F showed apparently uniform ink coverage to the naked eye, whereas those printed in ink G displayed obvious inhomogeneities, with considerable variations in print density across the page. These print irregularities could be traced to corresponding irregular image transfer on the plate and blanket, and thence to uneven transfer of ink throughout the inking train, despite reciprocation, leading to roll stripping on the form roller. This suggests an upper limit of about 100 Pa s at 40 s^{-1} for ceramic inks and hence a window within which inks giving sinterable printed densities (Table 2) can be formulated by judicious selection of dispersant and level of dilution with solvent. The lower limit was about 30 Pas as shown above.

It could be argued that since high shear rates are encountered in the inking train and in transfer to the plate and blanket cylinders, viscosity should be measured at high shear rates. There are two problems with this. Firstly, poor discrimination is achieved at high shear rates (Fig. 5). Secondly, one of the most important features of the ink that emerges in this study is the capacity for flow after transfer so that pin holes may be healed. This occurs at low shear rates.

Table 4
Ink and fountain settings used in printing test pages

Ink	Ink setting	Fountain setting
Commercial black	24°	14°
E	28°	14°
F	40°	14°
G	49°	18°

3.3. Resolution and gain of negative and plate

To assess the dimensional tolerance of the ceramic image, the accuracy of the test design at each stage of the platemaking process must be distinguished from individual ink properties. The feature resolution, at all stages from computer artwork to printing is summarised in Table 5. Line gap resolution is defined as the minimum gap in the artwork which gives no joins in the print between parallel lines each drawn 200 μm wide. Cavity resolution was the smallest clearly distinguishable square cavity. In the case of the computer artwork (row 1, Table 5), the resolution refers to the design file for the test pattern (Fig. 2); the smallest dimension allowed by the software was 10 μm. In transfer to the negative, resolution was lost, as were the smallest features. No further loss occurred on platemaking. It is a characteristic of transfer to negative that features were reduced by about 10 μm in the transverse direction and 4 μm in the longitudinal direction (Table 6). This partly offsets the expansion of about 10 μm in both directions on UV exposure of the plate which is due to diffraction at edges, poor collimation and lateral advance of the polymerisation front. There is a net uncompensated extension of features in the longitudinal axis of $\leqslant 8$ μm on the plate. In addition, features at the extremities of the negative were extended in both directions by up to 250 μm but this was confined to within 30 mm of the edge of the printing area. These effects of elongation and magnification limit the available area of the plate from which nominally identical components may be printed, unless the distortion is taken into account when the plate is designed and component dimensions are adjusted accordingly in the original design.

3.4. Continuity, resolution and gain of printed images

Images in commercial black ink and ceramic inks F and G were compared using optical and scanning electron microscopy (Figs. 7–9). The micrographs show regions from an interdigitated pattern of lines (Fig. 2) drawn 200 μm wide with 300 μm spacing (original artwork). Figs. 7a and 7b are optical and secondary electron images of the same region of the interdigitated pattern printed in commercial black ink. The opacity of the carbon-filled ink means that these images show a close correlation in feature shape and size. This is not the case for the translucent ceramic inks discussed below. The commercial ink forms an almost continuous film containing cavities; large irregular voids up to 80 μm across and smaller ovoid pores. These reflect the tendency for fountain to become entrained in the ink. They show no obvious orientation in the print direction and are typical of offset lithographic print.[45] There is negligible feathering at the ink-fountain interfaces. The incomplete surface coverage seen in Figs. 7 and 8 is not associated with substrate surface roughness; similar images were seen when printing onto smooth polyester sheet.

Figs. 8a and b show the equivalent region of interdigitation printed with ink F (37 vol.% ceramic). In this case, there is a discrepancy between the features resolved in optical and SEM images because the ink is

Table 5
Resolution of selected features in the test pattern

	Dot resolution (μm)	Line resolution (μm)	Cavity resolution (μm)	Line-gap resolution (μm)
Artwork	20	20	20	50
Negative	40	40	60	50
Plate	40	40	60	50
Commercial black	40	40	100	100
Ink E	40	40	80	50
Ink F	60	40	100	50
Ink G	60	40	100	50

Table 6
Variation in size of selected features in test pattern and gain during printing

	Transverse		Longitudinal	Dot area ($\mu m^2 \times 10^{-4}$)
	Line width (μm)	Dot width (μm)	Dot width (μm)	
Artwork	200	200	200	4
Negative	189	192	196	3.8
Plate	198	198	207	4.1
Commercial black	282	236	247	5.8
Ink E	216	216	220	4.8
Ink F	211	227	244	5.6
Ink G	208	212	222	4.7

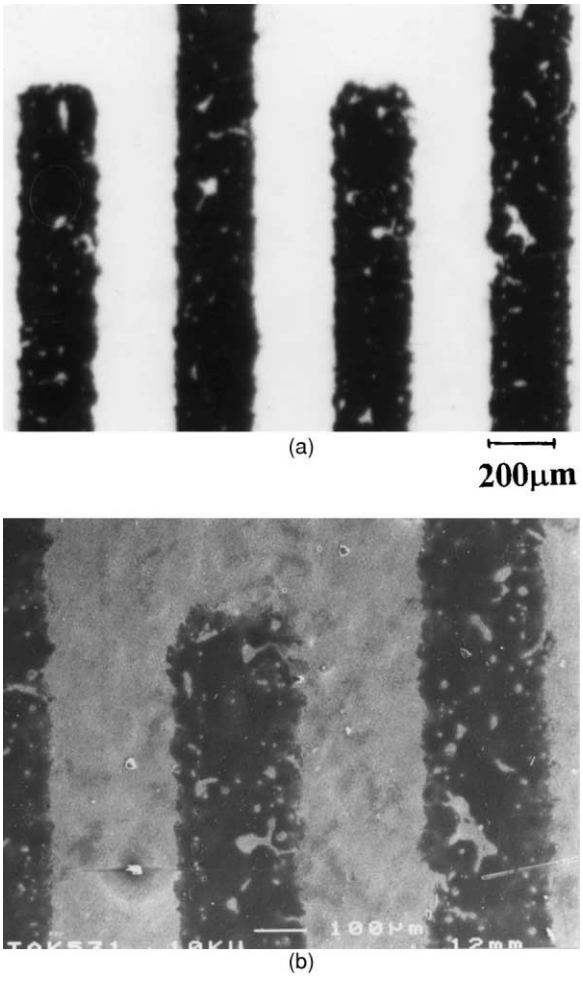

Fig. 7. (a) Bright field transmission optical micrograph of interdigitated pattern printed in commercial black ink. (b) Secondary scanning electron micrograph of the same region of interdigitated pattern printed in commercial black ink.

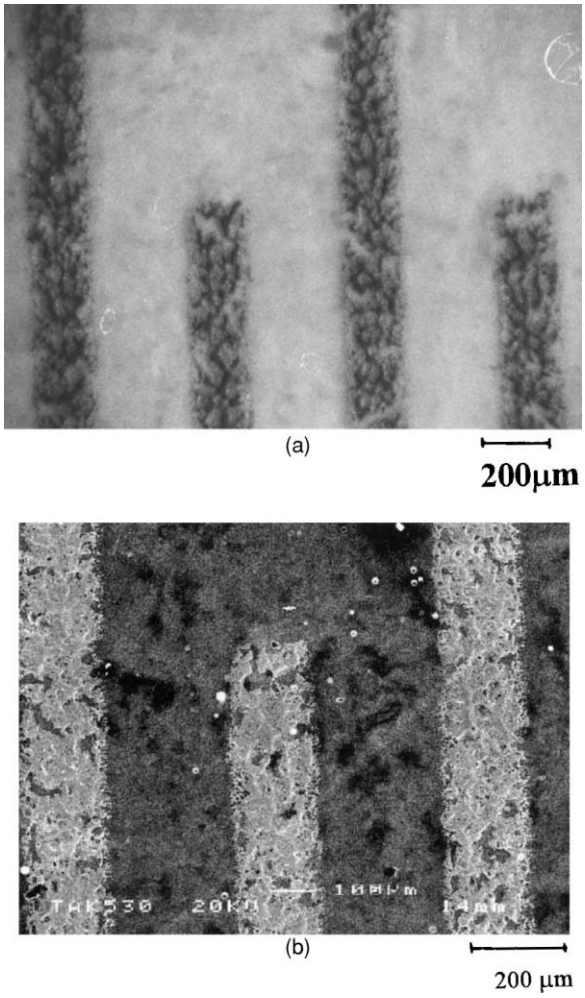

Fig. 8. (a) Bright field transmission optical micrograph of interdigitated pattern printed in ceramic ink F. (b) Secondary scanning electron micrograph of the same region of interdigitated pattern printed in ceramic ink F.

translucent, preventing resolution of thin regions in the optical microscope and significantly underestimating surface coverage. The ink displays finer microstructural features than that printed in the commercial black ink, with smaller pores, distinct feathering at the edges of the film and clear contours in film thickness. The overall coverage is somewhat lower and line and area gain are lower, more accurately reproducing the dimensions of the plate design. Feathering and contoured surfaces indicate that relative to the commercial black ink, ink F shows less self-levelling on the plate surface, owing to higher low shear-rate viscosity, (too high to measure in the cone and plate rheometer). The survival of structures formed during emulsification and film splitting depends on the thixotropic recovery time of the ink.

Fig. 9 shows an equivalent region printed with ink G (40 vol.% ceramic) and illustrates the effect of increasing the viscosity of the ink. Overall surface coverage is dramatically reduced and the ink has been deposited in the form of discrete islands, with little evidence of spreading. This is not simply a question of wettability; equilibrium contact angles are not achieved. It is associated with insufficient flow at low shear rates.

The main difference between the commercial and ceramic inks is the area coverage. The ceramic inks form strings and beads; a characteristic which becomes more pronounced as the ceramic loading and hence viscosity are increased. A smaller fraction of the image area is covered and thickness is variable. Pores are variable in both size and outline but the outline of the ink film closely follows the shape of the interdigitated structure. The boundary of large pores is clearly defined by a string of small ink beads. Feathering is seen along the edges of the ceramic ink films, consisting of chains of small, connected ink droplets. These features are consistent with the emulsification of the edges of the ink films, where they interacted with the fountain-coated non-printing regions of the plate.

Figs. 7 and 8 show the line and area gains and gap resolution. The black ink gives improved area coverage

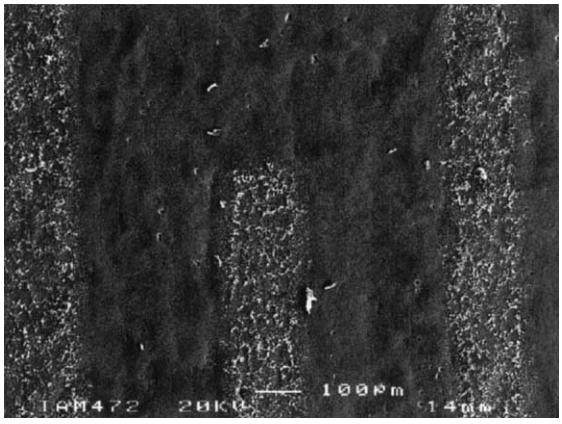

Fig. 9. Secondary scanning electron micrograph of the same region of interdigitated pattern printed in ceramic ink G.

at the expense of much higher gain and lower gap resolution. Line gain and dot dilation for the printed test pages are given in Table 6, together with the dimensions of the features in the original computer-generated artwork, the negative, plate and on the printed page. Line gain is taken as the absolute deviation in width from the dimensions on the plate. Lines drawn 200 μm wide in the original artwork, normal to the direction of paper travel through the press are again used as an arbitrary standard. Dot dilation is the deviation of width in directions normal and transverse to the direction of paper travel, from which area gain can be found.

The direction of paper travel had little effect on the spreading of ink. The commercial black ink consistently spread to a greater degree than the ceramic inks and formed more continuous films. The line gain observed for the ceramic inks was similar to their dot width dilations, but for the commercial black ink, it was about double the dot spread. This effect correlates with the observed greater homogeneity of the black ink film and its more complete coverage of the paper. This is mainly due to greater fluidity of the black ink under press conditions. The ceramic inks spread consistently during printing and then stabilise, without undergoing further self-levelling, while the black ink flows to give a more uniform thickness. This is consistent with the black ink having higher line thickness gain than dot width gain, while the ceramic inks display similar dilation of both features, a line providing a greater reservoir of ink for lateral spreading.

An important observation for the efficacy of this process is that the limit of resolution (size of the smallest dot that can be printed) is imposed chiefly by the plate resolution, rather than limitations imposed by the ink (Table 5). Resolution of non-printed areas (size of the smallest gap) is additionally affected by the spreading of the ink film and the level of porosity that it contains. Line-gap and cavity resolution in test pages printed with commercial black ink were limited by spreading of the ink film into the non-printed areas. The line gap was always resolved in ceramic inks, with no joins between lines being observed but cavity resolution was limited by a combination of ink spreading and porosity, it being impossible to distinguish very small cavities in the test pattern from pores in the surrounding ink film.

3.5. Multiple pass overprinting

The Multilith press relies on manual adjustment of the register board and the jogger guide to achieve registration and therefore registration errors in this work should not be seen as inherent in the process. Overprinting (without drying) up to five times with the commercial black ink resulted in consistent increases in image density, but resolution and continuity were limited by registration and transfer of partly dried ink by the paper feed mechanism. Surface coverage was limited by the tendency of layers of ink already printed to be pulled off the page during the printing of successive layers. Like the black ink, ceramic ink E (35 vol.%) showed a higher image density but pinholes were not entirely eliminated. Ink F (37 vol.%) behaved in a similar way. Repeated overprinting with ink G (40 vol.%), while generally increasing print density, also resulted in the irregular transfer of ink from the page back onto the plate, leaving characteristic scratch marks parallel to the direction of paper travel.

In an attempt to alleviate the problem of ink pull-off, test pages were overprinted two and five times with an extended drying period (29 ks) between passes. Fig. 10 shows the area coverage for two layers of ink E. A few pinholes of about 10 μm diameter remain. After five such layers (Fig. 11) the number of pinholes is reduced and even at high magnification it is not possible to conclude that they penetrate to the substrate. Although coverage is almost complete, the paper substrate is dimensionally unstable on repeated wetting and drying.

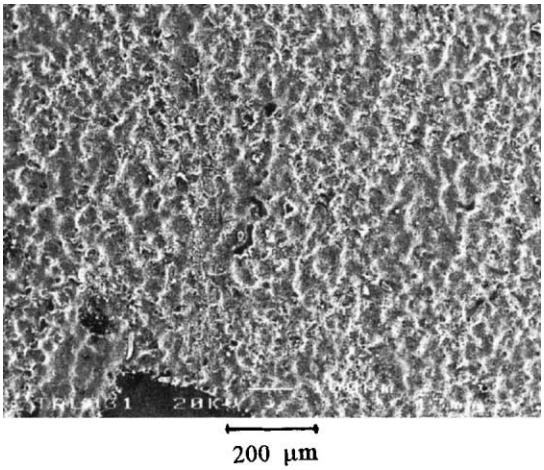

Fig. 10. Secondary scanning electron micrograph of circular area overprinted in two layers of ceramic ink E, with 29 ks drying time between layers. The larger cavity at the bottom of the figure is part of the test pattern design.

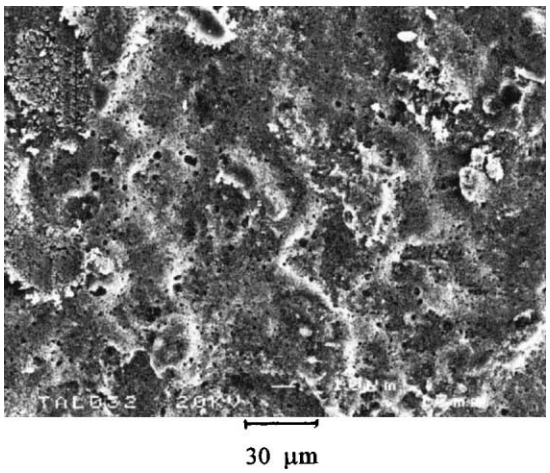

Fig. 11. Secondary scanning electron micrograph of circular area overprinted in five layers of ceramic ink E, with 29 ks drying time between layers.

Absorption of fountain solution during printing causes the paper to swell, and upon drying it exhibits shrinkage of up to 0.2%, rendering adequate registration of detailed patterns impossible. Such problems are avoided when printing onto dense polymeric films.

Addressing now the post printing treatments, there are two alternatives. On the one hand, such ceramic-polymer films could be used in situ in conjunction with the conducting tracks previously described.[16–20] In this context the applications might include, 0–3 piezoelectric composites, resistors, thermistors, capacitors, photoresistors and various sensors. The final ceramic volume fraction is then given in Table 2 and is partly dependent on the solvent-resin ratio.

In another context, the multiple layer devices could be removed from the substrate and sintered. A film of ink E (35 vol.% ceramic drying to 53 vol.%), about 100 μm thick was pyrolysed at 5°C/h to 450°C in air and sintered at 1350°C for 2 h. The fracture surface (Fig. 12) shows residual porosity within grains as a result of discontinuous grain growth. This suggests the presence of a siliceous or glassy phase perhaps collected from the organic vehicle.

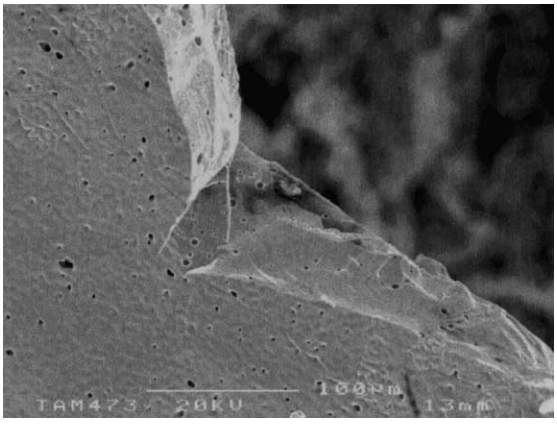

Fig. 12. Secondary scanning electron micrograph of fracture surface of thin film of ceramic ink E sintered at 1350°C for 7.2 ks.

A sample of organic vehicle was therefore pyrolysed to 650°C in air. It left a grey fluffy deposit which was shown by energy dispersive X-ray analysis to contain Co, La, Ce, Si and Mg in approximate order of abundance. Some of these impurities arise from the ink drier. The purity of ink vehicle will be examined more extensively in future work.

4. Conclusions

This paper has demonstrated the viability of offset lithographic printing for fine (200 nm) ceramic powder at volume loadings up to 40 vol.% drying to 58 vol.%. The best print quality was obtained with a 35 vol.% ink drying to 53 vol.%. Selection of dispersant at the 2 mg m^{-2} level based on the powder BET area was critical for fluidity of inks, varying over one order of magnitude for different but related dispersants.

Rheological characterisation of printing ink was experimentally challenging because of long thixotropic relaxation times, the tendency for cavitation in the cone and plate rheometer and high viscosity at low shear rate. Since steady-state is not reached during printing, efforts to record steady state viscosities, sometimes taking up to 11 ks, are open to the charge of irrelevance, while rapid sweeps can produce almost any flow curve in inks showing rheopexy.

Emulsification of ceramic ink using the Surland test showed a strong dependence of water uptake on viscosity. The validity of the Surland test as a predictor of print quality is questionable when the ink characteristics differ significantly from those of reprographic inks for which it was designed.

When the ink viscosity (ceramic or commercial ink) was below 26 Pa s at a shear rate of 40 s^{-1}, the ink was not printable but instead emulsified and covered the non-printing areas. A ceramic ink having a viscosity of 350 Pa s at 40 s^{-1} (deduced by extrapolation) produced a low surface coverage and discontinuous print quality and this sets an approximate upper limit.

The smallest feature resolution when printing on highly calendered paper was 40 μm which matched the resolution of the platemaking process. The cavity resolution was 80 μm, compared to 60 μm for the plate manufacture. Resolution in multiple layer printing was limited by manual mechanical adjustment and by paper dilation and shrinkage. These limitations would be avoided on high performance machines and when printing on to polymer film. Surface coverage was consistently improved by multiple overprinting after 29 ks drying time between layers.

Acknowledgements

The authors are grateful for EPSRC funding under grant no. GR/MO6093 and to Martin Thompson of Coates-Lorilleux for helpful advice and supply of materials.

References

1. Willoughby, C. and Evans, J. R. G., The manufacture of laminated ceramic composites using paint technology. *J. Mater Sci.*, 1996, **31**, 2333–2337.
2. Kim, H. Y. and Kim, H., Microstructural control during photosensitive ceramic thick film processing. *J. Ind. Eng. Chem.*, 1998, **4**, 78–83.
3. Blazdell, P. F., Evans, J. R. G., Edirisinghe, M. J., Shaw, P. and Binstead, M. J., The computer aided manufacture of ceramics using multilayer jet printing. *J. Mater. Sci. Lett.*, 1995, **14**, 1562–1565.
4. Xiang, Q. F., Evans, J. R. G., Edirisinghe, M. J. and Blazdell, P. F., Solid freeforming of ceramics using a drop on demand jet printer. *J. Eng. Manufact.*, 1997, **211B**, 211–214.
5. Mott, M. and Evans, J.R.G. Zirconia/alumina functionally graded material made by inkjet printing, *Mater. Sci. Eng. A*, 1999, **A271**, 344–352.
6. Yao, K. and Zhu, W. G., Improved preparation procedure and properties for a multilayer piezoelectric thick-film actuator. *Sensors and Actuators*, 1998, **A71**, 139–143.
7. Lauder, A., Cima, M. J., Sachs, E. and Fan, T., Three dimensional printing: surface finish and microstructure of rapid prototyped components. *Mater. Res. Soc. Symp. Proc.*, 1992, **249**, 331–336.
8. Atkinson, A., Doorbar, J., Hudd, A., Segal, D. L. and White, P. J., Continuous ink-jet printing using sol-gel ceramic' inks. *J. Sol-Gel Sci. Technol.*, 1997, **8**, 1093–1097.
9. Song, J. H., Edirisinghe, M. J. and Evans, J. R. G., Formulation and multilayer jet printing of ceramic inks. *J. Am. Ceram. Soc.*, 1999, **82**, 3374–3380.
10. Slade, C. E. and Evans, J. R. G., Freeforming ceramics using a thermal inkjet printer. *J. Mater. Sci.*, 1998, **17**, 1669–1671.
11. Wright, M. J. and Evans, J. R. G., Ceramic deposition using an electromagnetic jet printer station. *J. Mater. Sci. Lett.*, 1999, **18**, 99–101.
12. Seerden, K. A. M., Reis N., Derby, B., Grant P.S., Halloran, J.W. and Evans, J. R. G., Direct inkjet deposition of ceramic green bodies; I formulation of build materials. In *Solid Freeform and Additive Fabrication*, MRS Symp. Proc. Vol. 542, ed. D. Dimos, S. C. Danforth and M. J. Cima. Warrendale, PA, 141–146, (1999).
13. Reis, N., Seerden, K. A. M., Derby, B., Halloran, J. W., and Evans, J. R. G., Direct inkjet deposition of ceramic green bodies: II. Jet behaviour and deposit formation. In *Solid Freeform and Additive Fabrication*, MR Symp. Proc., Vol. 542, ed. D. Dimos, S. C. Danforth and M. J. Cima, MRS, Warrendale, Pennsylvania, USA, 147–152 (1999).
14. Mott, M., Song, J. H. and Evans, J. R. G., Microengineering of ceramics by direct inkjet printing. *J. Am. Ceram. Soc.*, 1999, **82**, 1653–1658.
15. Ruud, N., The metal printing process: solid freeform fabrication of an object in metal. *Conf. on Materials Opportunities in Layered Manufacturing Technologies*. Abingdon UK, June 1998.
16. Harrison, D., Billett, E., and Billingsley, E., Int. Conf. On Clean Electronics. PNC. IEE/IEEE, 1995, pp. 174–76.
17. Ramsey, B. J., Evans, P. S. A. and Harrison, D., A novel circuit fabrication technique using offset lithography. *J. Electronic Manufact.*, 1997, **7**, 63–67.
18. Walton, A. J., Stevenson, J. T. M., Haworth, L. I., Fallon, M., Evans, P. S. A., Ramsey, B. J. and Harrison, D., Characterisation of offset lithographic films using microelectronic test structures. *IEICE Transactions on Electronics*, 1999, **E82C**, 576–581.
19. Shepherd, P. R., Evans, P. S. A., Ramsey, B. J. and Harrison, D. J., Lithographic technology for microwave integrated circuits. *Electronics Lett.*, 1997, **33**, 483–484.
20. Evans, P. S. A., Ramsey, B. J., Harrey, R. M. and Harrison, D. J., Printed analogue filter structures. *Electronics Lett.*, 1999, **35**, 306–308.
21. Leach, R. H., Pierce, R. J., Hickman, E. P., Mackenzie, M. J., and Smith, H. G., *The Printing Ink Manual*, 5th edn. Chapman and Hall London, 1993, pp. 342–452.
22. Newnham, R. E., Skinner, D. P. and Cross, L. E., Connectivity and piezoelectric-pyroelectric composites. *Mater. Res. Bull.*, 1978, **13**, 525–536.
23. Surland, A., A laboratory method for prediction of lithographic ink performance. *TAGA Conference Proceedings*, vol. 32, pp. 222-247 Williamsburg, PA, USA.
24. Bagley, E. B., Dintzies, F. R. and Chakrabarti, S., Experimental and conceptual problems in the rheological characterisation of wheat flour doughs. *Rheol. Acta*, 1998, **37**, 556–563.
25. Volz J., A Practical Method for Testing Litho Properties of Ink, *American Inkmaker*, February 1998, pp. 42–45.
26. Kendall, J. and Monroe, K. P., The viscosity of liquids II. The viscosity: compositon curve for ideal liquid mixtures. *J. Am. Chem. Soc.*, 1917, **38**, 1787–1802.
27. Kendall, J. and Monroe, K. P., The viscosity of liquids V. The ideality of the system: Benzene-Benzyl Benzoate and the validity of the Bingham fluidity formula. *J. Am. Chem. Soc.*, 1921, **43**, 114–125.
28. Alexander, D. M. and Moy, D. C., The viscosity of Liquid Mixtures. *Aust. J. Chem.*, 1981, **34**, 1573–1577.
29. Shankar, P. N. and Kumar, M., Experimental determination of the kinematic viscosity of glycerol-water mixtures. *Proc. Roy. Soc. Lond.*, 1994, **A444**, 537–581.
30. Moloney, V. M. B., Parris, D. and Edirisinghe, M. J., Rheology of zirconia suspensions in a non-polar organic medium. *J. Am. Ceram. Soc.*, 1995, **78**, 3225–3232.
31. Song, J. H. and Evans, J. R. G., Ultrafine ceramic powder moulding: the role of dispersants. *J. Rheol.*, 1996, **40**, 131–152.
32. Simpson, P., Testing control and quality assurance. In *The Printing Ink Manual*, 5th edn. ed. R. H. Leach and R. J. Pierce. Chapman and Hall, London, 5th edn. 1993, pp. 804–864.
33. Private communication Van Son Corp^{n}. Technical Information Dept., 30 September 1999.
34. Tabernor, G. A., Rheology of printing inks. In *The Printing Ink Manual*, 5th Edn. ed. R. M. Leach and R. J. Pierce. Kluwer Academic, Dordrecht, The Netherlands, 1993, p. 784.
35. McKelvey, J. M., *Polymer Processing*. Wiley, New York, USA, 1962 pp. 211–227.
36. Gregory, T. and Mayers, S., A note on slippage during the study of the rheological behaviour of paste inks. *JOCCA — Surface Coatings International*, 1993, **76**, 82–86.
37. Coussot, P., Leonov, A. A. and Piau, J. M., Rheology of concentrated dispersed systems in a low molecular weight matrix. *J. Non-Newtonian Fluid Mech.*, 1993, **46**, 179–217.
38. Mas, R. and Magnin, A., Rheology of colloidal suspensions: case of lubricating greases. *J. Rheol.*, 1994, **38**, 889–908.
39. Nakai, Y., Ryo, Y. and Kawaguchi, M., Transient and steady-state rheology of silica suspensions in hydroxypropyl(methyl)cellulose solutions. *Chem. Soc. Faraday Trans.*, 1993, **89**, 2467–2472.
40. Watanabe, H., Yao, M.-L., Yamagishi, A., Osaki, K., Shitata, T., Niwa, H. and Morishima, Y., Nonlinear rheological behavior of a concentrated spherical silica suspension. *Rheol. Acta*, 1996, **35**, 433–445.
41. de Rooji, R., Potanin, A. A., van den Ende, D. and Mellema, J., Transient shear viscosity of weakly aggregating polystyrene latex dispersions. *J. Chem. Phys.*, 1994, **100**, 5353–5360.
42. West, A. H. L., Melrose, J. R. and Ball, R. C., Computer simulations of the breakup of colloid aggregates. *Physical Review E*, 1994, **49**, 4237–4249.
43. Cheng, D., Thixotropy. *Int. J. Cosmetic Sci.*, 1987, **9**, 151–191.
44. Leach, R. H., Pierce, R. J., Hickman, E. P., Mackenzie, M. J. and Smith, H. G., *The Printing Ink Manual*, 5th edn. Chapman and Hall, London, 1993, p. 366.
45. Leach, R. H., Pierce, R. J., Hickman, E. P., Mackenzie, M. J. and Smith, H.G., *The Printing Ink Manual*, 5th edn. Chapman and Hall, London. 1993 p 78.